

**Best
Available
Copy**

AD-A284 994

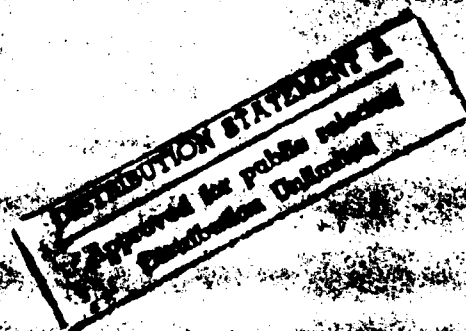


ABSORPTION ANALYSIS APPLIED TO NEUTRONS
IN A THERMAL COLUMN

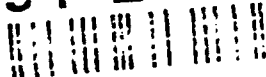
L. F. Lowe
E. A. Burke



November 1960



94-23542



94 7 26 032

ELECTRONICS RESEARCH DIRECTORATE
AIR FORCE CAMBRIDGE RESEARCH LABORATORIES
AIR RESEARCH AND DEVELOPMENT COMMAND
UNITED STATES AIR FORCE
BEDFORD, MASSACHUSETTS

Requests for additional copies by Agencies of the Department of Defense, their contractors, and other government agencies should be directed to the:

Armed Services Technical Information Agency
Arlington Hall Station
Arlington 12, Virginia

Department of Defense contractors must be established for ASTIA services, or have their 'need-to-know' certified by the cognizant military agency of their project or contract.

All other persons and organizations should apply to the:

U. S. DEPARTMENT OF COMMERCE
OFFICE OF TECHNICAL SERVICES,
WASHINGTON 25, D. C.

Question For	
DTIC GRA&I	<input checked="checked" type="checkbox"/>
DTIC TAB	<input type="checkbox"/>
Unannounced	<input type="checkbox"/>
Justification	
By	
Date/Location	
Availability Codes	
Dist	Avail and/or Special
A-1	

AFCRL-TR-60-355

ABSORPTION ANALYSIS APPLIED TO NEUTRONS
IN A THERMAL COLUMN

L. F. Lowe
E. A. Burke

Project 5620
Task 56208

November 1960

ELECTRONIC MATERIAL SCIENCES LABORATORY
ELECTRONICS RESEARCH DIRECTORATE
AIR FORCE CAMBRIDGE RESEARCH LABORATORIES
AIR RESEARCH AND DEVELOPMENT COMMAND
UNITED STATES AIR FORCE
BEDFORD, MASSACHUSETTS

ABSTRACT

The energy spectrum of diffuse neutrons in the thermal column of the MIT reactor has been determined by analyzing transmission data. The results are compared to a Maxwellian distribution and to a previous experiment done on collimated thermal neutrons.

Accession For	
NTIS GRA&I	<input checked="" type="checkbox"/>
DTIC TAB	<input type="checkbox"/>
Unannounced	<input type="checkbox"/>
Justification	
By	
Distribution/	
Availability Codes	
Dist	Avail and/or Special
A-1	

Submitted for publication 24 October 1960.

ACKNOWLEDGMENT

The authors gratefully acknowledge the following: Walter B. Jackson, Bartholomew J. Spada and George W. Johanson for the design and fabrication of the various pieces of equipment necessary to carry out this experiment; J. P. Cali and Joseph R. Weiner for the boron analysis; Professor Shull of MIT for the use of the neutron monochromator; Raymond Ehrenbeck for the design of the split die and the MIT reactor staff for their assistance in carrying out this experiment.

TABLE OF CONTENTS

	Page
Abstract	iii
Acknowledgment	v
Introduction	1
Theoretical Procedure	1
Experimental Procedure	4
Results	6
Conclusion	7
References	9
Appendix 1	10
Appendix 2	12
Appendix 3	16

ABSORPTION ANALYSIS APPLIED TO NEUTRONS IN A THERMAL COLUMN

INTRODUCTION

It has been shown (see reference 1 and Appendix 1), that the energy spectrum of a collimated neutron beam can be derived from transmission data. This report will describe the application of this method to the more general case of diffuse neutrons.

THEORETICAL PROCEDURE

The case of a collimated neutron beam will first be discussed and then the appropriate changes necessary to convert this to the diffuse case will be developed. In reference to Figs. 1 and 4, if $f(E)$ represents the neutron flux per energy interval, $\sigma(E)$ the activation cross section for the gold detector, $\Sigma_T(E)$ the total cross section for the absorbing material, and x the absorber thickness, then the activity, $A(x)$, imparted to the gold detector would be

$$A(x) = K \int_0^{\infty} e^{-\Sigma_T(E)x} \sigma(E) f(E) dE \quad (1)$$

where K is a constant.

Figure 1 shows the geometry used for the diffuse case. Graphite spheres borated with varying amounts of boron were used. Therefore, instead of increasing the thickness, x , of the absorber, the total cross section Σ_T was increased by adding more boron.

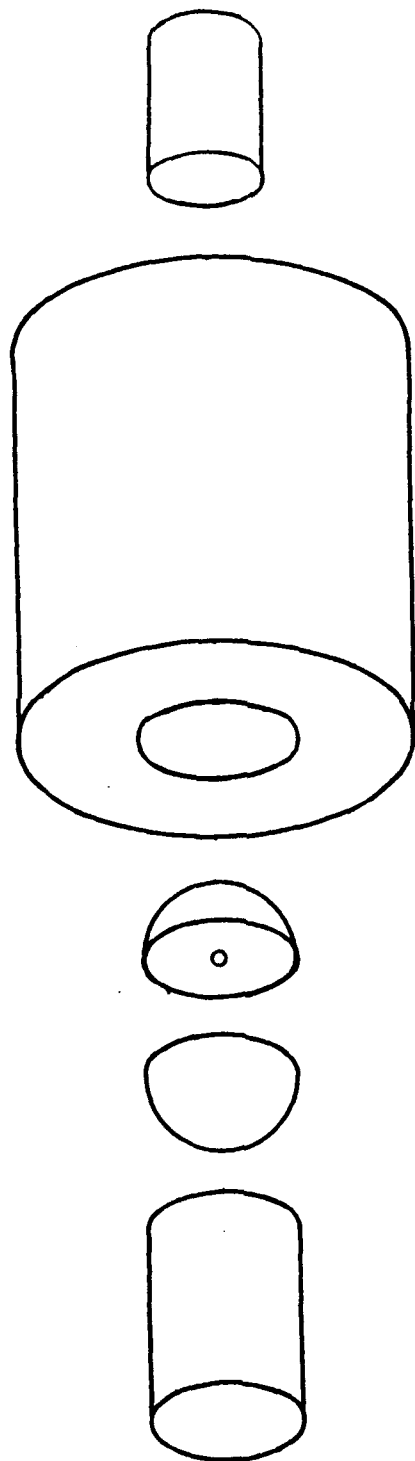


Figure 1. The Experimental Setup

As can be seen from Fig. 1, a neutron may reach the gold detector by more than one path. Hence, the attenuation factor which was $e^{-\Sigma_T(E)x}$ for the beam case is now more complicated, namely,

$$\int_0^{\infty} e^{-\Sigma_T(E)x} P(x) dx \quad (2)$$

where $P(x)$ is the fraction of neutrons that travel the distance x per x interval. Fortunately, it was found (see Appendix 2) that this attenuation factor could be represented to a good approximation by a simple exponential,

$$\int_0^{\infty} e^{-\Sigma_T(E)x} P(x) dx \cong K e^{-\Sigma_T(E)\bar{x}} \quad (3)$$

where \bar{x} can be considered as an equivalent distance through which the average neutron passes, and K is a constant.

Now Eq. (1) can be rewritten for the diffuse case as

$$A(B) = K \int_0^{\infty} e^{-\Sigma B} \sigma(E) f(E) dE \quad (4)$$

where

$$\Sigma = \frac{\sigma_B(E)N}{A_B} \quad (5)$$

$$B = \rho \bar{x} b \quad (6)$$

where the quantities $\sigma_B(E)$, N , A_B , ρ , and b are defined as the microscopic total cross section for boron, Avogadro's number, the atomic weight of boron, the

sphere's density, and the weight fraction of boron, respectively. It should be noted that the quantity B has the dimensions of grams cm^{-2} , which makes it suitable for a transmission curve, and also that Σ does not have its usual meaning and is independent of the boron concentration.

Now, since Σ , $\sigma(E)$, and $f(E)$ are all functions of E , we can define a new quantity, $\phi(\Sigma)$, such that

$$\phi(\Sigma) d\Sigma = \sigma(E) f(E) dE \quad (7)$$

If we now substitute Eq. (7) into Eq. (4), we obtain

$$A(B) = -K \int_0^{\infty} e^{-\Sigma B} \phi(\Sigma) d\Sigma \quad (8)$$

which involves the assumption that $\Sigma = 0$ for $E = \infty$, and $\Sigma = \infty$ for $E = 0$.

Equation (8) now has the form of a Laplace transform and hence, if $A(B)$ is determined experimentally, $\phi \Sigma$ can be obtained from the inverse transform of $A(B)$.

The desired quantity, $f(E)$, is then obtained by use of Eq. (7);

$$f(E) = \frac{\phi(\Sigma)}{\sigma(E)} \left(\frac{d\Sigma}{dE} \right) \quad (9)$$

EXPERIMENTAL PROCEDURE

Figure 1 shows the experimental setup. A gold detector was placed in the center of the two borated hemispheres. This was held in a graphite cylinder which was inserted into a graphite stringer for the irradiation with thermal neutrons at the MIT reactor. Six inches above the sphere, another graphite cylinder containing a gold detector was inserted. This acted as a flux monitor.

The activity, $A(B)_i$ of the i^{th} gold ball within the i^{th} borated sphere would be given by

$$A(B)_i = N(B)_i S_i \Phi(B)_i \int_0^{\infty} e^{-\Sigma B} \phi(\Sigma) d\Sigma \quad (10)$$

where $N(B)_i$ is the number of gold atoms in the i^{th} detector, S_i is the activation saturation term, and $\Phi(B)_i$ is the flux at the detector.

The activity $A(m)_i$ of the i^{th} monitor would be

$$A(m)_i = N(m)_i S_i \Phi(m)_i \bar{\sigma} \quad (11)$$

where $N(m)_i$ is the number of gold monitor atoms, $\Phi(m)_i$ is the flux at the monitor, and $\bar{\sigma}$ is the average activation cross section for gold.

What we actually measured was the ratio of Eq. (10) to Eq. (11) which would be

$$\frac{A(B)_i}{A(m)_i} = R(B) = \frac{N(B)_i S_i \Phi(B)_i \int_0^{\infty} e^{-\Sigma B} \phi(\Sigma) d\Sigma}{N(m)_i S_i \Phi(m)_i} \quad (12)$$

Equation (12) simplifies to

$$R(B) = \frac{W(B)_i}{W(m)_i} \frac{F}{\bar{\sigma}} \int_0^{\infty} e^{-\Sigma B} \phi(\Sigma) d\Sigma \quad (13)$$

where $\frac{W(B)_i}{W(m)_i}$ is the weight ratio which would be equal to the atom ratio, and

F is the ratio of the fluxes with no boron present

$$F = \frac{\Phi(B)_0}{\Phi(m)_0} = \frac{A(B)_0}{W(B)_0} \frac{W(m)_0}{A(m)_0} \quad (14)$$

Equation (13) can be rewritten

$$\frac{R(B) W(m)_i}{F W(B)_i} = P(B) = \int_0^{\infty} e^{-\Sigma B} \phi(\Sigma) d\Sigma \quad (15)$$

With no boron present, $P(B)$ would be

$$P(O) = \frac{R(O)W(m)_o \bar{\sigma}}{F W(B)_o} = \bar{\sigma} \quad (16)$$

Therefore, in order to make $P(O) = 1$, we define $Q(B)$ as

$$Q(B) = \frac{P(B)}{\bar{\sigma}} = \int_0^{\infty} e^{-\Sigma B} \theta(\Sigma) d\Sigma \quad (17)$$

where

$$\theta(\Sigma) = \frac{\phi(\Sigma)}{\bar{\sigma}} \quad (18)$$

Finally, the desired quantity, $f(E)$, would be given by

$$f(E) = \frac{\theta(\Sigma) \bar{\sigma}}{\sigma(E)} \frac{d\Sigma}{dE} \quad (19)$$

where $\theta(\Sigma)$ is the inverse Laplace transform of the experimentally determined quantity $Q(B)$, and the other factors are obtained from known cross-section data for boron and gold.²

As can be seen from Eq. (17) and (15), one needs to know the ratio of the activities, $R(B)$, in order to calculate $Q(B)$. This was determined by placing the irradiated detectors and monitors into a scintillation well counter and measuring the ratio of their respective count rates, which should equal the ratio of their activities. This ratio should also be independent of time.

RESULTS

Table 1 shows $Q(B)$ along with the values of B for the various spheres (see Appendix 3). The transform $T(B)$ yielded the best fit to $Q(B)$. $T(B)$ is given by

$$T(B) = e^{-n(\sqrt{B+d} - \sqrt{d})} \quad (20)$$

where a and d were found to be 16.76 and 0.0256, respectively. This transform is also found in Table 1.

The inverse transform of Eq. (20) is

$$\theta(\Sigma) = \frac{ae^{a\sqrt{d}}}{2\sqrt{\pi}} e^{-d\Sigma} e^{-a^2/4\Sigma} \Sigma^{-3/2} \quad (21)$$

Now $f(E)$ can be obtained from Eq. (21) with the use of Eq. (19). This is shown compared to a Maxwellian flux distribution at 293°K in Fig. 2.

CONCLUSION

Previous experience¹ has shown that this method should be valid within 10 percent. However, as can be seen from Fig. 2, the experimentally determined spectrum differs from the Maxwellian distribution by greater than 10 percent. There are at least four possible explanations for this fact:

1. The neutrons in the MITR thermal column have the energy distribution as found, within 10 percent.
2. The mathematical analysis of the problem, especially the scattering part thereof, may be in error to a degree.
3. The positioning of the spheres relative to the monitors was not done with sufficient accuracy.
4. The flux gradient between the sphere and the monitor did not remain constant throughout the experiment.

Of the possibilities, 3 and 4 seem the most probable, since this experiment was carried out over a three-week period which involved ten separate irradiations.

However, it appears that the method of absorption analysis can be applied to the diffuse case, and it certainly could be improved by changing the experimental setup so as to ensure constant geometry and perhaps eliminate the scattering problem.

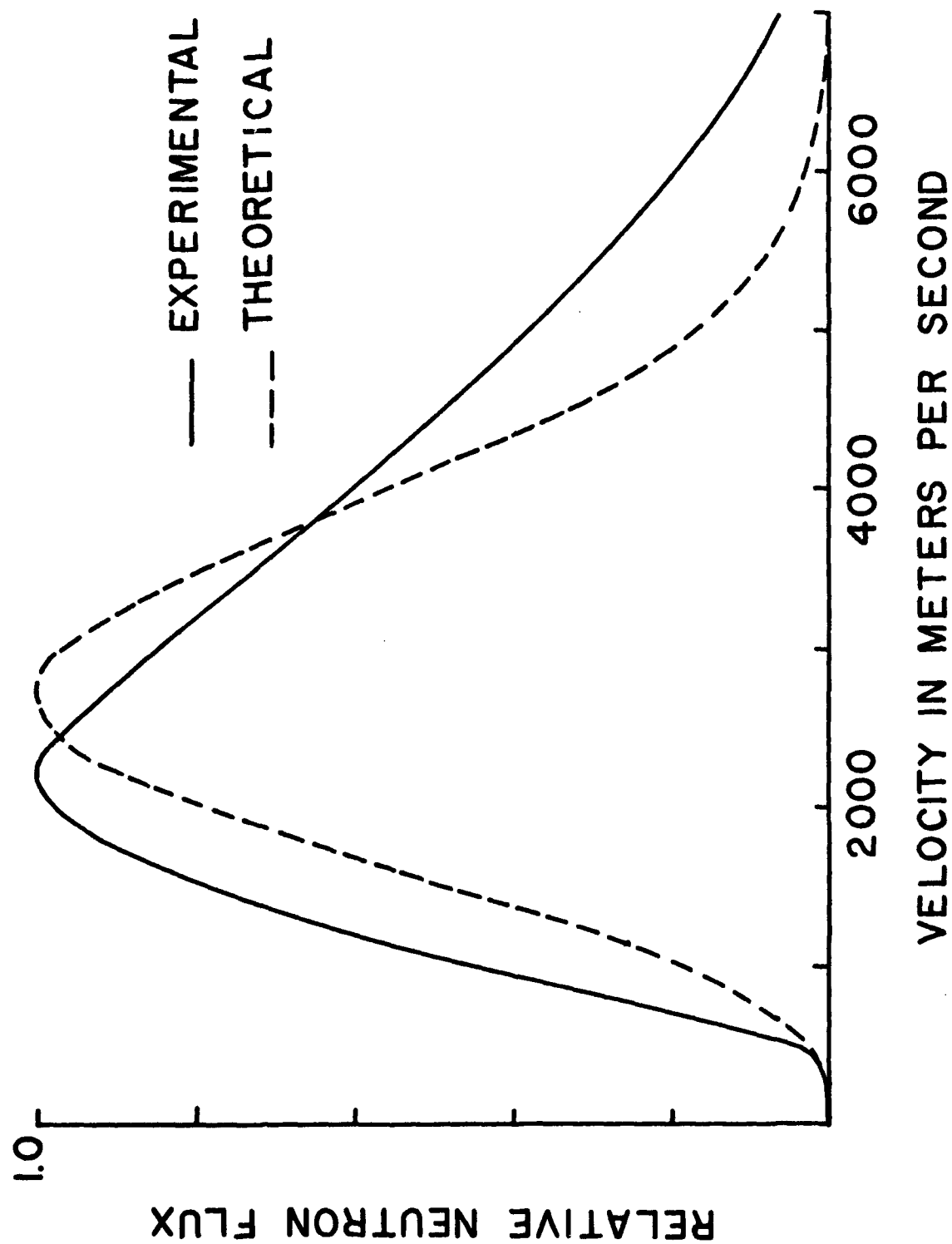


Figure 2 Experimental and Maxwellian Distributions Compared for the Diffuse Case

REFERENCES

1. E. A. BURKE and L. F. LOWE, Nuclear Instruments and Methods, 7, 193-196 (1960).
2. D. J. HUGHES and R. B. SCHWARTZ, BNL-325.

APPENDIX 1

ABSORPTION ANALYSIS ON A COLLIMATED NEUTRON BEAM

For the collimated case, silver absorbers of thickness x were used, with a boron trifluoride tube as the neutron detector. The absorption curve obtained is shown in Table 2 along with the transform fit. The transform that yielded this fit was

$$T(x) = e^{[b\sqrt{c} - b\sqrt{x+c} - ax]} \quad 1.1$$

Equation 1.1 yielded the inverse transform,

$$\theta(\Sigma) = \begin{cases} 0 & \text{when } (\Sigma - a) < 0 \\ \frac{b}{2\pi(\Sigma - a)^{3/2}} e^{[b\sqrt{c} - c(\Sigma - a) - \frac{b^2}{4(\Sigma - a)}]} & \text{when } (\Sigma - a) > 0 \end{cases} \quad 1.2$$

where the values of a , b and c were found to be 1.30, 3.31 and 0.31, respectively.

In order to obtain the neutron flux distribution from $\phi(\Sigma)$, it must be multiplied by $\frac{d\Sigma}{dV}$ and divided by the energy-dependent detector efficiency. The result thus obtained is shown compared to a Maxwellian at 293°K in Fig. 3.

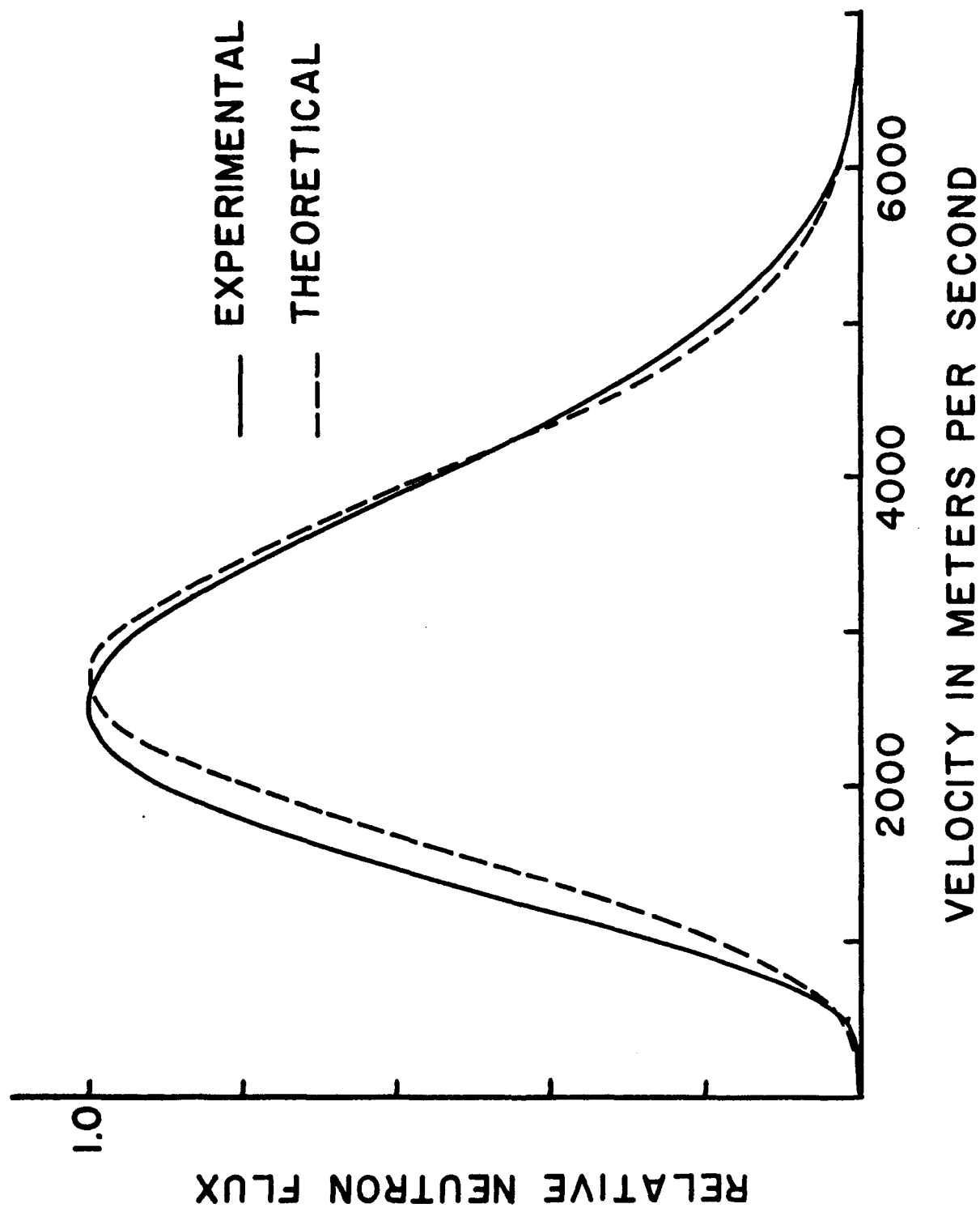


Figure 3. Experimental and Maxwellian Distributions Compared for the Collimated Case

APPENDIX 2

DETERMINATION OF THE SCATTERING CORRECTION FACTORS

Calculation will be made of the effective length that the neutrons must pass through to reach the gold detector at the center of the sphere. The results obtained here will show that the neutron attenuation is exponential with respect to the total cross section. Thus, the neutrons act as if they were travelling through 1.062 cm of absorber in a 1.000-cm radius sphere. This simple exponential property allows us to use the Laplace transform technique to solve the integral equation.

Figure 4 shows the geometry for this problem. Let us consider an elemental volume in this figure. The number of neutrons that reach it from a unit area on the surface would be

$$\left(\frac{\phi_0}{4}\right) \frac{e^{-\Sigma_T x}}{2\pi x^2} = \phi(x, \theta) \quad 2.1$$

where ϕ_0 is the diffuse flux at the surface, and Σ_T is the total macroscopic cross section of the sphere. The quantity $\phi(x, \theta)$ would be the neutron current at the point x for a given θ . Now if Σ_S is the macroscopic scattering cross section, then $\phi(x, \theta)\Sigma_S$ would be the number of scattered neutrons per second per unit volume. If we now multiply this quantity by the number of unit volumes dv , we have

$$df = \phi(x, \theta)\Sigma_S dv \quad 2.2$$

where df is the differential number of neutrons being scattered per second per differential volume. Combining Eq. 2.1 and 2.2 we get

$$df = \left(\frac{\phi_0}{4}\right) \frac{e^{-\Sigma_T x}}{2\pi x^2} \Sigma_S dv \quad 2.3$$

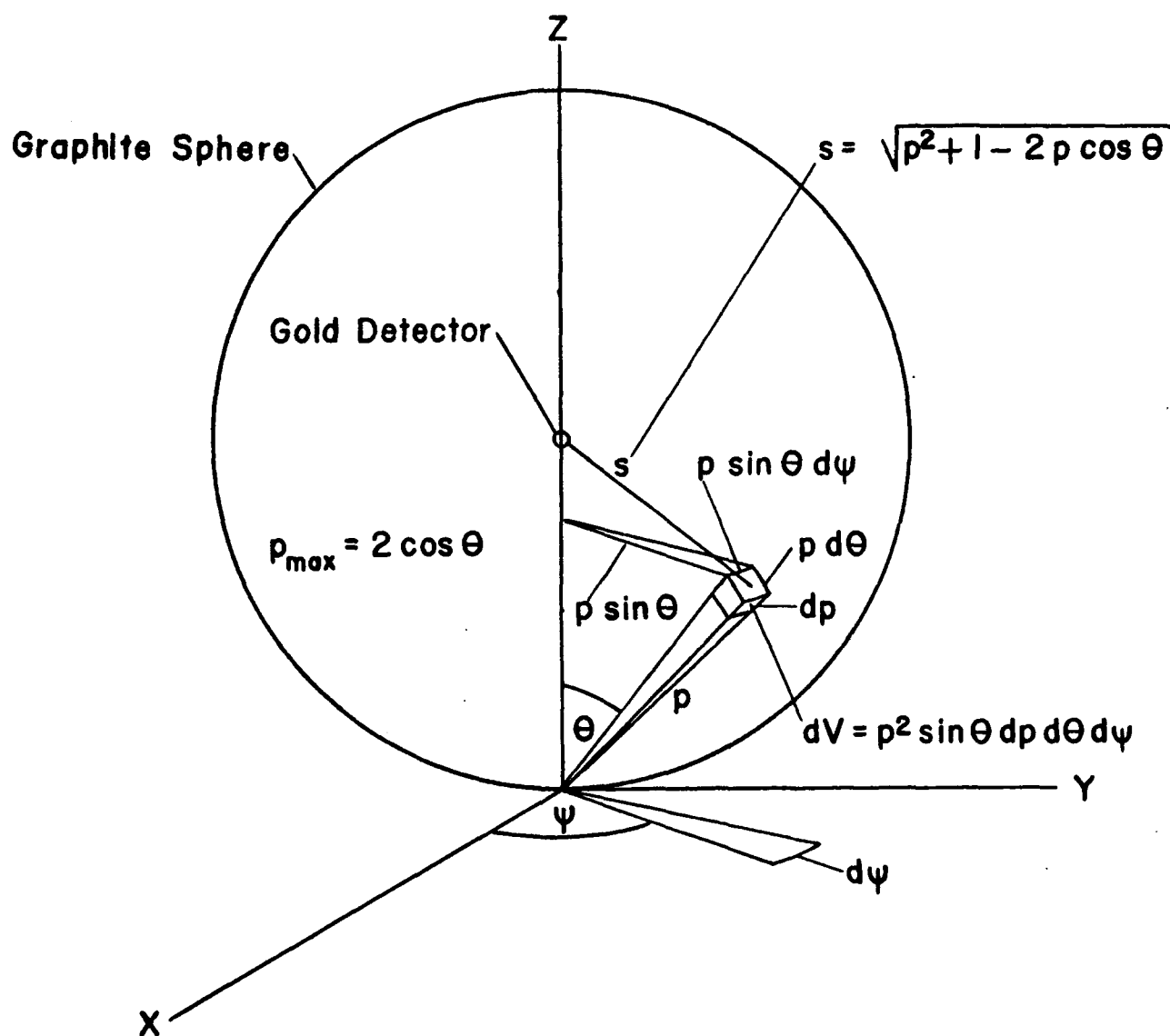


Figure 4. The Scattering Geometry

From Fig. 4, dv would be

$$dv = x^2 \sin \theta dx d\theta d\psi \quad 2.4$$

Combining Eqs. 2.3 and 2.4, we get

$$df = \frac{\phi_0}{8\pi} e^{-\Sigma_T x} \Sigma_S \sin \theta dx d\theta d\psi \quad 2.5$$

The neutrons at df must travel the distance y in order to reach the center. Therefore, the differential flux, dn , at the center would be

$$dn = \frac{e^{-\Sigma_T y}}{4\pi y^2} df \quad 2.6$$

From Fig. 4

$$y = \sqrt{x^2 + 1 - 2x \cos \theta} \quad 2.7$$

Now by combining Eqs. 2.5, 2.6 and 2.7 we get

$$dn = \frac{\phi_0 \Sigma_S e^{-\Sigma_T (x + \sqrt{x^2 + 1 - 2x \cos \theta})} \sin \theta dx d\theta d\psi}{32\pi^2 (x^2 + 1 - 2x \cos \theta)} \quad 2.8$$

In order to obtain the total flux, N , at the center, due to the entire surface, we must multiply by $4\pi r^2 = 4\pi$ and integrate, thereby obtaining

$$N = \frac{\phi_0 \Sigma_S}{8\pi} \int_{x=0}^{2\cos\theta} \int_{\theta=0}^{\pi/2} \int_{\psi=0}^{2\pi} \frac{e^{-\Sigma_T (x + \sqrt{x^2 + 1 - 2x \cos \theta})} \sin \theta dx d\theta d\psi}{(x^2 + 1 - 2x \cos \theta)} \quad 2.9$$

Since the integration with respect to ψ amounts to multiplication by 2π and $\Sigma_S = 0.48 \text{ cm}^{-1}$, we now have

$$N = 0.12\phi_0 \int_{x=0}^{2\cos\theta} \int_{\theta=0}^{\pi/2} \frac{e^{-\Sigma_T(x + \sqrt{x^2 + 1 - 2x\cos\theta})} \sin\theta \, dx \, d\theta}{(x^2 + 1 - 2x\cos\theta)} \quad 2.10$$

Since this N represents the neutron current at the center, for activation purposes, $2N$ must be used.

Unfortunately, Eq. 2.10 cannot be evaluated analytically. Graphical methods must be used. The results of this double graphical integration are shown in Table 3. The flux at the center due to primary scattering is represented by ϕ_S , ϕ_d represents the straight in component, and ϕ_T the flux at the center due to ϕ_S and ϕ_d . The value of ϕ_T at $\Sigma_T(0.50)$ corresponds to no boron. This shows that the direct-in plus the primary scattered neutrons account for 92.3 percent of the neutrons at the center. The remaining 7.7 percent would be due to multiply-scattered neutrons. This 7.7 percent is too large to ignore, and since it cannot be calculated conveniently at other values of Σ_T , it is estimated to drop off at the same rate as the primary. This is equivalent to multiplying the primary contribution by 1.247 to give now the total contribution at the center due to scattering, designated as ϕ_{ST} and tabulated along with ϕ_{TT} which is now $\phi_{ST} + \phi_d$.

It was found that ϕ_{TT} could be represented by a simple exponential

$$\phi_{TT} = e^{-1.062(\Sigma_T - 0.5)} \quad 2.11$$

APPENDIX 3

DETERMINATION OF BORON

The borated spheres were made by mixing known amounts of reactor grade graphite powder with purified boron powder. After shaking on a paint mixer for 15 minutes, the samples were subjected to a pressure of 12 tons per square inch to form a solid borated graphite rod. From this rod two 1-cm hemispheres were machined and used to hold the gold ball as shown in Fig. 1.

The percentage of boron was determined by three different methods: 1) the weights used; 2) chemical analysis of the mixed powder; and 3) neutron transmission analysis of the hemispheres.

The chemical analysis was made by converting the boron to boric acid, complexing the boric acid so as to make it a strong acid, and then titrating with standard hydroxide.

The neutron transmission analysis was carried out at the MIT reactor using a collimated beam of monoenergetic neutrons and determining the percent transmission for the various hemispheres. Since these neutrons had an energy of 0.0806 electron volts, for which boron has a total cross of 422 barns, the quantity B is given by

$$B = \frac{\bar{x} A}{N \sigma} \ln \frac{1}{T} = 0.04255 \bar{x} \ln \frac{1}{T} \quad 3.1$$

where A is the atomic weight of boron, N is Avogadro's number, σ is the microscopic absorption cross section of boron, and T is the transmission.

The results of the three methods are shown in Table 4. As can be seen, the claim of 99.2 percent for the purity of the boron seems to be a bit high. The transmission analysis data, the only method which actually would take into account the cross sections of any possible impurities in the hemispheres, was used.

TABLE 1
VALUES OF Q(B), T(B), and B

Sphere	B (grams/cm ²)	Q(B)	T(B)
1	0	1.000	1.000
2	0.00417	0.804	0.814
3	0.0118	0.579	0.574
4	0.0174	0.448	0.455
5	0.03099	0.272	0.271
6	0.0471	0.172	0.161
7	0.0655	0.0776	0.093
8	0.08232	0.0593	0.0600
9	0.1049	0.0346	0.0346
10	0.1296	0.0205	0.0199

TABLE 2

COMPARISON OF $T(x)$ WITH THE EXPERIMENTAL ABSORPTION DATA
FOR THE COLLIMATED CASE

x (cm)	Absorption Curve	$T(x)$
0.0000	1.000	1.000
0.0230	0.908	0.907
0.0591	0.783	0.783
0.1322	0.586	0.586
0.1811	0.491	0.491
0.238	0.399	0.399
0.324	0.297	0.297
0.430	0.209	0.209
0.622	0.1152	0.1150
0.795	0.0691	0.0693
0.952	0.0446	0.0445
1.190	0.0230	0.0233
1.365	0.0148	0.0148

TABLE 3
VALUES OF ϕ_S , ϕ_d , ϕ_T , ϕ_{TT} , ϕ_{ST} , and Σ_T

$\Sigma_T (\text{cm}^{-1})$	ϕ_S	ϕ_d	ϕ_T	ϕ_{ST}	ϕ_{TT}
0.50	0.316	0.606	0.923	0.394	1.000
1.20	0.1344	0.301	0.435	0.168	0.419
2.50	0.0275	0.0820	0.1095	0.0343	0.1163
4.00	0.00502	0.0183	0.0233	0.00625	0.02455
6.00	0.000556	0.00249	0.00305	0.000695	0.00318

TABLE 4
VALUES OF b FROM DIFFERENT ANALYSES

Sphere	Weights (Assuming 0.992 Purity)	Chemical Analysis	Neutron Transmission Analysis
2	0.00212	0.0019	0.00185
3	0.00556	0.0049	0.0052
4	0.00820	0.0076	0.0075
5	0.0151	0.0144	0.01374
6	0.0227	0.0216	0.02084
7	0.0322	0.0306	0.02945
8	0.0402	0.0378	0.03735
9	0.05145	0.0505	0.0483
10	0.0628	0.0592	0.0599

<p>AD</p> <p>AF Cambridge Research Laboratories, Bedford, Mass.</p> <p>ABSORPTION ANALYSIS APPLIED TO NEUTRONS IN A THERMAL COLUMN, by L. F. Lowe and E. A. Burke. November 1960. 19p. incl. illus. (Proj. 5620; Task 56208) (AFRL-TR-60955) Unclassified report</p> <p>The energy spectrum of diffuse neutrons in the thermal column of the MIT reactor has been determined by analyzing transmission data. The results are compared to a Maxwellian distribution and to a previous experiment done on collimated thermal neutrons.</p>	<p>UNCLASSIFIED</p> <p>1. Neutron spectra, determination of</p> <p>2. Thermal neutrons</p> <p>3. Absorption analysis</p> <p>I. Lowe, L. F.</p> <p>II. Burke, E. A.</p>	<p>AD</p> <p>AF Cambridge Research Laboratories, Bedford, Mass.</p> <p>ABSORPTION ANALYSIS APPLIED TO NEUTRONS IN A THERMAL COLUMN, by L. F. Lowe and E. A. Burke. November 1960. 19p. incl. illus. (Proj. 5620; Task 56208) (AFRL-TR-60955) Unclassified report</p> <p>The energy spectrum of diffuse neutrons in the thermal column of the MIT reactor has been determined by analyzing transmission data. The results are compared to a Maxwellian distribution and to a previous experiment done on collimated thermal neutrons.</p>	<p>UNCLASSIFIED</p> <p>1. Neutron spectra, determination of</p> <p>2. Thermal neutrons</p> <p>3. Absorption analysis</p> <p>I. Lowe, L. F.</p> <p>II. Burke, E. A.</p>	<p>UNCLASSIFIED</p> <p>1. Neutron spectra, determination of</p> <p>2. Thermal neutrons</p> <p>3. Absorption analysis</p> <p>I. Lowe, L. F.</p> <p>II. Burke, E. A.</p>
<p>AD</p> <p>AF Cambridge Research Laboratories, Bedford, Mass.</p> <p>ABSORPTION ANALYSIS APPLIED TO NEUTRONS IN A THERMAL COLUMN, by L. F. Lowe and E. A. Burke. November 1960. 19p. incl. illus. (Proj. 5620; Task 56208) (AFRL-TR-60955) Unclassified report</p> <p>The energy spectrum of diffuse neutrons in the thermal column of the MIT reactor has been determined by analyzing transmission data. The results are compared to a Maxwellian distribution and to a previous experiment done on collimated thermal neutrons.</p>	<p>UNCLASSIFIED</p> <p>1. Neutron spectra, determination of</p> <p>2. Thermal neutrons</p> <p>3. Absorption analysis</p> <p>I. Lowe, L. F.</p> <p>II. Burke, E. A.</p>	<p>AD</p> <p>AF Cambridge Research Laboratories, Bedford, Mass.</p> <p>ABSORPTION ANALYSIS APPLIED TO NEUTRONS IN A THERMAL COLUMN, by L. F. Lowe and E. A. Burke. November 1960. 19p. incl. illus. (Proj. 5620; Task 56208) (AFRL-TR-60955) Unclassified report</p> <p>The energy spectrum of diffuse neutrons in the thermal column of the MIT reactor has been determined by analyzing transmission data. The results are compared to a Maxwellian distribution and to a previous experiment done on collimated thermal neutrons.</p>	<p>UNCLASSIFIED</p> <p>1. Neutron spectra, determination of</p> <p>2. Thermal neutrons</p> <p>3. Absorption analysis</p> <p>I. Lowe, L. F.</p> <p>II. Burke, E. A.</p>	<p>UNCLASSIFIED</p> <p>1. Neutron spectra, determination of</p> <p>2. Thermal neutrons</p> <p>3. Absorption analysis</p> <p>I. Lowe, L. F.</p> <p>II. Burke, E. A.</p>

AD	UNCLASSIFIED	AD	UNCLASSIFIED
	UNCLASSIFIED		UNCLASSIFIED
AD	UNCLASSIFIED	AD	UNCLASSIFIED
	UNCLASSIFIED		UNCLASSIFIED